Relationship between Three-Dimensional Arrays of "Lipidic Particles" and Bicontinuous Cubic Lipid Phases†

Leif Rilfors,*,‡ Per-Olof Eriksson,‡ Gösta Arvidson,§ and Göran Lindblom‡

Department of Physical Chemistry, University of Umeå, S-901 87 Umeå, Sweden, and Department of Physiological Chemistry, University of Uppsala, Biomedical Centre, S-751 23 Uppsala, Sweden

Received February 19, 1986; Revised Manuscript Received June 12, 1986

ABSTRACT: Several lipid–water mixtures form phases that give rise to freeze–fracture replicas exhibiting three-dimensional regular arrays of closely packed globular elements, often called "lipidic particles". These phases have often been poorly classified with respect to long-range organization and symmetry and have in most cases been asserted to be built up by closed lipid aggregates, such as reversed micelles. However, studies of phases giving rise to the above-mentioned freeze–fracture replicas, with X-ray diffraction and the nuclear magnetic resonance pulsed field gradient diffusion technique, have revealed that they are (1) *cubic* liquid-crystalline phases and (2) with one exception *bicontinuous* phases, i.e., cubic phases in which both the hydrocarbon and the water regions are continuous. Up to now the only known exception is a cubic phase composed of closed rod-shaped micelles of the *normal* type. Thus it is not possible to decide from a freeze–fracture image of a cubic phase, showing three-dimensional arrays of "lipidic particles", if the phase is bicontinuous or composed of closed lipid aggregates. Hitherto, it has not been shown that a biological membrane lipid–water system is able to form a cubic liquid-crystalline phase consisting of reversed micelles. The existence of such a phase is also improbable considering the location in the phase diagrams of cubic phases formed by biological membrane lipid–water systems.

The occurrence of "lipidic particles" in freeze–fracture replicas of liposome suspensions was first reported 7 years ago (Verkleij et al., 1979). Subsequent studies of this phenomenon have revealed that "lipidic particles" can be organized in several ways (Verkleij, 1984): randomly arranged single particles, rows of particles, and two-dimensional or three-dimensional arrays of particles. The formation of "lipidic particles" in lipid–water mixtures has attracted much attention, since these structures have been proposed to be involved in processes such as membrane fusion and transport of proteins, lipids, and polar solutes across membranes (De Kruijff et al., 1985).

A three-dimensional regular array of "lipidic particles" is formed by several lipid–water mixtures: (1) mixtures of one lipid and water, such as monoglyceride–water and egg lysophosphatidylcholine (LPC)–water[1] (Gulik-Krzywicki et al., 1984); (2) mixtures of two lipids and water, such as monogalactosyldiacylglycerol (MGalDG)–digalactosyldiacylglycerol (DGalDG)–water (Sen et al., 1981, 1982; Sprague & Staehelin, 1984), phosphatidylcholine (PC)–phosphatidylethanolamine (PE)–water (Hui & Boni, 1982; Hui et al., 1983; Boni & Hui, 1983), and monoglucosyldiacylglycerol (MGluDG)–diglucosyldiacylglycerol (DGluDG)–water (Verkleij, 1984); and (3) mixtures of one or two lipids, water, and cholesterol, a divalent cation, or a local anesthetic; examples of these mixtures are PC–cholesterol–water (Dekker et al., 1983), egg PC–diphosphatidylglycerol (DPG)–Ca^{2+}–water (Van Venetië & Verkleij, 1981), DPG–dibucaine–water (Cullis et al., 1978), and phosphatidic acid–chlorpromazine–water (Verkleij et al., 1982). It should also be mentioned that freeze–fracture replicas with three-dimensional arrays of "lipidic particles" have been obtained from lipid–water mixtures both below (Gulik-Krzywicki et al., 1984) and above [for example, Sen et al. (1982) and Hui et al. (1983)] maximum hydration of the lipids and at temperatures from 0 (Cullis et al., 1978) to 80 °C (Dekker et al., 1983).

Freeze–fracture electron micrographs showing three-dimensional arrays of "lipidic particles" have been interpreted to represent (1) a cubic phase built up of reversed spherical micelles (Boni & Hui, 1983), (2) quasi-crystalline or crystallike arrangements of reversed micelles (Sen et al., 1981, 1982; Verkleij, 1984), (3) conglomerates or agglomerates of reversed micelles (Van Venetië & Verkleij, 1981; Verkleij et al., 1982), or (4) "regions of short reversed hexagonal phase" (Cullis et al., 1978). Consequently, the lipid–water phases yielding the above-mentioned freeze–fracture images have often been poorly classified with respect to long-range organization and symmetry (descriptions 2, 3, and 4). However, *all* these descriptions of the phase structures have one feature in common: the phase structures are asserted to be built up of closed lipid aggregates of the reversed type, i.e., structures with discontinuous water regions and with continuous hydrocarbon regions. By X-ray diffraction studies the monoglyceride–water phase (Lindblom et al., 1979; Longley & McIntosh, 1983; Larsson, 1983; Gulik-Krzywicki et al., 1984) and the

† This work was supported by the Swedish Natural Science Research Council, the K. and A. Wallenberg Foundation, the Wenner-Gren Foundation, "Stiftelsen Bengt Lundqvists Minne", the Carl Trygger Foundation, and the Magnus Bergvall Foundation.

‡ University of Umeå.

§ University of Uppsala.

[1] Abbreviations: PC, phosphatidylcholine; POPC, 1-palmitoyl-2-oleoylphosphatidylcholine; DOPC, dioleoylphosphatidylcholine; LPC, lysophosphatidylcholine; LaLPC, 1-lauroyl-*sn*-glycero-3-phosphocholine; OlLPC, 1-oleoyl-*sn*-glycero-3-phosphocholine; PE, phosphatidylethanolamine; DOPE, dioleoylphosphatidylethanolamine; DLiPE, dilinoleoylphosphatidylethanolamine; DPG, diphosphatidylglycerol; MGalDG, monogalactosyldiacylglycerol; DGalDG, digalactosyldiacylglycerol; MGluDG, monoglucosyldiacylglycerol; DGluDG, diglucosyldiacylglycerol; C_{12}TACl, dodecyltrimethylammonium chloride; FT, Fourier transform; NMR, nuclear magnetic resonance; H_I, normal hexagonal phase; H_{II}, reversed hexagonal phase; Tris, tris(hydroxymethyl)aminomethane; EDTA, ethylenediaminetetraacetic acid.

0006-2960/86/0425-7702$01.50/0

MGalDG–DGalDG–water phase (Rivas & Luzzati, 1969; Brentel et al., 1985) have been classified as cubic liquid-crystalline phases according to the established classification applied to lyotropic liquid-crystalline systems (Luzzati & Tardieu, 1974). Moreover, with the nuclear magnetic resonance (NMR) pulsed field gradient diffusion technique, it has been shown that these cubic phases are bicontinuous (Lindblom et al., 1979; Brentel et al., 1985). In such a cubic phase the lipid aggregates building up the phase are connected to each other, i.e., both the hydrocarbon and the water regions are continuous. Freeze–etching electron microscopy investigations of the monoglyceride–water system have given support for a bicontinuous structure of this cubic phase (Gulik-Krzywicki et al., 1984).

In this work we show with the NMR diffusion technique that two lipid–water mixtures, giving rise to freeze–fracture replicas with three-dimensional arrays of "lipidic particles", form bicontinuous cubic liquid-crystalline phases. The structures of cubic phases previously obtained with biological membrane lipids, as well as the structures of cubic phases with different locations in the phase diagrams of lipid–water mixtures, are discussed.

Background

It has long been known that translational diffusion in lipid–water systems can be studied with the NMR pulsed field gradient technique [see, for example, Charvolin & Rigny (1971), Bull & Lindman (1974), Roeder et al. (1976), Lindblom & Wennerström (1977), Kuo & Wade (1979), Stilbs et al. (1984), and Stilbs (1986)]. The main advantage of this method is that the diffusion coefficient can be measured directly; i.e., no probe molecule has to be used, and no model-dependent assumptions have to be made. Furthermore, one is able to vary the time during which the diffusion is measured, and in this work the chosen diffusion times correspond to molecular root-mean-square displacements of $\approx$1 and $\approx$10 μm for lipids and water, respectively. *Thus one measures molecular displacements over distances much larger than the dimension of a single micelle* (Figure 1).

From a comparison of lipid translational diffusion coefficients in cubic and lamellar liquid-crystalline phases and of the diffusion coefficients of water in cubic phases and in pure water, it is possible to distinguish between two fundamentally different types of cubic phases (Lindblom & Wennerström, 1977; P.-O. Eriksson, G. Lindblom, and G. Arvidson, submitted for publication): (1) structures with continuous regions of both water and hydrocarbon chains (Luzzati et al., 1968; Scriven, 1976; Lindblom et al., 1979); (2) structures, either with discontinuous hydrocarbon regions but with continuous water regions ("oil-in-water" structure) (Bull & Lindman, 1974; Eriksson et al., 1982; Eriksson et al., submitted for publication) or with discontinuous water regions but with continuous hydrocarbon regions ("water-in-oil" structure).

In bicontinuous cubic phases, diffusion of lipid molecules can occur over *macroscopical* distances without polar groups passing through hydrocarbon regions or without hydrocarbon chains passing through water regions (Figure 1). The measured lipid diffusion coefficient for such phases is therefore of the same order of magnitude as that obtained for the corresponding lamellar phase (Lindblom et al., 1979). Examples of this are given in Table I with the systems monoolein–water and 1-oleoyl-*sn*-glycero-3-phosphocholine (OlLPC)–water. Likewise, if the measured diffusion coefficient of water in a cubic phase is comparable to that of free water, the water regions are continuous (see Results and Discussion).

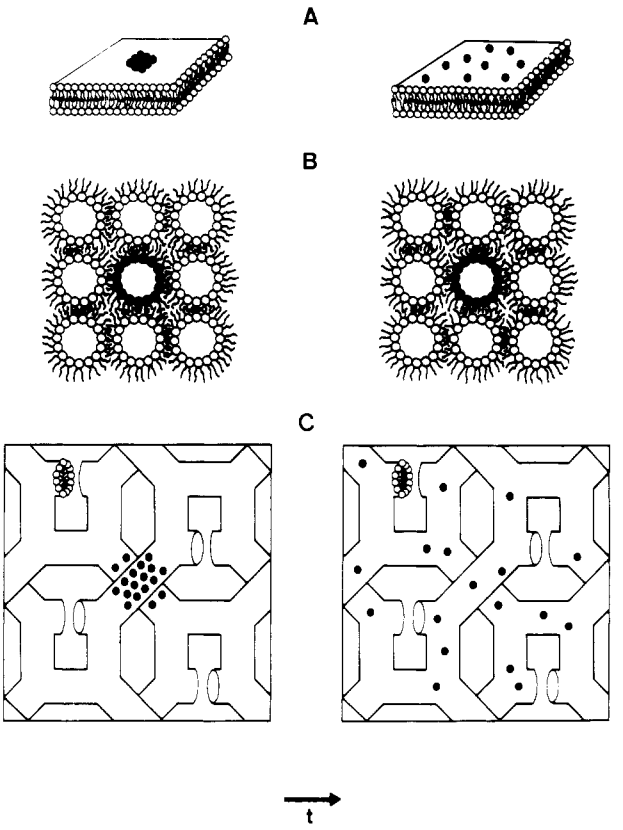

FIGURE 1: Illustration of the lipid translational diffusion in lipid–water phases of different structures during a time of milliseconds. (A) Lamellar phase. The lipids move freely in the aggregate plane and are able to transverse over large distances. The diffusion coefficient measured in the NMR experiment is the lateral diffusion coefficient D^{lam}. (B) A hypothetical cubic phase built up of reversed micelles. The lipids move freely *within* the aggregates, whereas interaggregate motion is hindered by hydrophobic interaction. The diffusion coefficient measured by NMR is considerably smaller than the lateral diffusion coefficient. The same reasoning is valid for a cubic phase built up of normal micelles. (C) Bicontinuous cubic phase built up of rod-shaped aggregates according to Luzzati et al. (1968). The lipids move freely along the aggregates, which are connected to each other. Therefore, the diffusion coefficient measured by NMR (D^{cub}) is of the same order of magnitude as the lateral diffusion coefficient. For clarity the rods are here drawn thinner than in the actual structure, where the length of the rods barely exceeds their diameter.

For cubic phases composed of closed aggregates, the lipid molecules can move freely within the aggregates, but it is very unlikely that they exchange between adjacent aggregates (Lindblom & Wennerström, 1977). Although the *local* molecular diffusion might be the same as in a lamellar aggregate, the *measured* diffusion coefficient is between 1 and 2 orders of magnitude lower (Figure 1) for such cubic phases than for the corresponding lamellar phase (Lindblom & Wennerström, 1977; Eriksson et al., submitted for publication). This is exemplified in Table I with the systems OlLPC–water (84 wt % OlLPC) and sodium octanoate–decanol–water on the one hand and the systems 1-lauroyl-*sn*-glycero-3-phosphocholine (LaLPC)–water and sodium octanoate–octane–water on the other hand, of which the latter systems form cubic phases consisting of closed aggregates of the normal type ("oil-in-water") (Lindblom & Wennerström, 1977; Eriksson et al., submitted for publication).

A comparison of the lipid translational diffusion coefficients in cubic phases consisting of closed aggregates and bicontinuous cubic phases is also shown in Table I. The cubic phases obtained with the sodium octanoate–octane–water system, the LaLPC–water system, and the dodecyltrimethylammonium

Table I: Measured and Calculated Values for the Lipid Translational Diffusion Coefficient in Surfactant–Water and Biological Lipid–Water Systems[a]

sample	compn (wt %)	phase	temp (°C)	$D^{lam} \times 10^{12}$ ($m^2 \cdot s^{-1}$)	$D^{cub} \times 10^{12}$ ($m^2 \cdot s^{-1}$)	$D_L^{cub} \times 10^{12}$ ($m^2 \cdot s^{-1}$)	$D_\parallel^{cub} \times 10^{12}$ ($m^2 \cdot s^{-1}$)
surfactants							
sodium octanoate[b]	22	lamellar	24	210			
decanol	40						
^2H_2O	38						
sodium octanoate[b]	39.4	cubic	24		1		
octane	4.3						
^2H_2O	56.3						
potassium octanoate[b]	65.0	cubic	24		88	130	260
^2H_2O	35.0						
$C_{12}TACl$[c]	50.1	cubic	29		0.5		
^2H_2O	49.9						
$C_{12}TACl$[c]	84.0	cubic	29		5	7.5	15
^2H_2O	16.0						
biological lipids							
monoolein[d]	88	lamellar	43	23[e]			
^2H_2O	12						
monoolein[d]	88	cubic	43		15	23	45
^2H_2O	12						
LaLPC[f]	40	cubic	29		0.06		
^2H_2O	60						
OlLPC[f]	84	lamellar	26	6			
^2H_2O	16						
OlLPC[f]	80	cubic	29		1.6	2.4	4.8
^2H_2O	20						
DOPC[g]	80	lamellar	20	2.8			
^2H_2O	20		40	7.5			

[a] D^{lam}, the measured lipid lateral diffusion coefficient in a lamellar phase; D^{cub}, the measured lipid translational diffusion coefficient in a cubic phase; D_L^{cub} and $D_\parallel^{cub}$, the calculated lipid translational diffusion coefficient in a bicontinuous cubic phase consisting of lamellar aggregates and rodlike aggregates, respectively. For explanation of the calculated diffusion coefficients, see Lindblom and Wennerström (1977) and Lindblom et al. (1979). [b] From Lindblom and Wennerström (1977). [c] From Bull and Lindman (1974). [d] From Lindblom et al. (1979). [e] Extrapolated from measurements in the lamellar phase formed at temperatures lower than 43 °C. [f] From P.-O. Eriksson, G. Lindblom, and G. Arvidson, submitted for publication. [g] From Lindblom et al. (1981). The value at 20 °C is extrapolated.

chloride ($C_{12}TACl$)–water system at high water content are composed of closed lipid aggregates; the cubic phases formed by potassium octanoate–water, OlLPC–water, and the $C_{12}TACl$–water mixture at low water content are bicontinuous (Bull & Lindman, 1974; Lindblom & Wennerström, 1977; Eriksson et al., 1982, submitted for publication). This comparison demonstrates that the measured lipid diffusion coefficients in the bicontinuous cubic phases are between 1 and 2 orders of magnitude higher than in the cubic phases consisting of closed lipid aggregates.

Materials and Methods

Sample Preparation. Dioleoylphosphatidylcholine (DOPC) and 1-palmitoyl-2-oleoylphosphatidylcholine (POPC) were prepared according to the method of Gupta et al. (1977). Dioleoylphosphatidylethanolamine (DOPE) was obtained from DOPC by phospholipase D catalyzed transphosphatidylation essentially as described by Comfurius and Zwaal (1977). A commercial preparation of phospholipase D (Sigma Chemical Co., St. Louis, MO) was used as enzyme source. The lipids were purified by column chromatography on silicic acid followed by treatment with decolorizing charcoal. Only trace amounts of contaminants could be detected by thin-layer chromatography analysis of the lipids. Dilinoleoylphosphatidylethanolamine (DLiPE) was purchased from Avanti Polar Lipids (Birmingham, AL), and bovine heart DPG (sodium salt) and dibucaine hydrochloride were purchased from Sigma. The purity of DLiPE and DPG was ≥99% as judged by thin-layer chromatography analysis, and they were used without further purification. Monoolein, technical grade (98% monoglyceride), was obtained from Grindsted Products, Brabrand, Denmark.

Lipid–water samples intended for investigations of the phase equilibria were prepared according to earlier descriptions (Eriksson et al., 1985a). For preparation of the DPG–dibucaine–^2H_2O samples heavy water containing 50 mM Tris–acetic acid (p^{2}H 7.2), 100 mM NaCl, and 2 mM EDTA was used (Cullis et al., 1978), and for preparation of the DLiPE–POPC–^2H_2O samples heavy water containing 100 mM NaCl was used (Boni & Hui, 1983). In the samples prepared for measurements of the lipid translational diffusion coefficient, the exchangeable protons in the amphiphilic molecules were removed by freeze-drying the samples after suspending the molecules in ^2H_2O. This process was repeated 3 times. After the last freeze-drying procedure the final amount of ^2H_2O was added and mixed thoroughly with the lipids. After NMR spectroscopy the samples were reanalyzed by thin-layer chromatography. About 2–3% of the lipids were found to be degraded in the DOPC–DOPE–^2H_2O samples, which had been heated to 80–90 °C, while no decomposition was noted in the DPG–dibucaine–^2H_2O samples. About 5–7% of the lipids were degraded in the DLiPE–POPC–^2H_2O samples.

NMR Measurements. ^{31}P NMR spectra were obtained either with a Bruker WM 250 or with a Bruker MSL 100 FT NMR spectrometer operating at 101.3 and 40.5 MHz, respectively. Inverse-gated high-power broad-band proton decoupling was applied, and an exponential multiplication corresponding to a 10-Hz line broadening was applied to the free

induction decays before Fourier transformation.

Translational diffusion coefficients were measured with the NMR pulsed magnetic field gradient technique (Stejskal & Tanner, 1965; Lindblom & Wennerström, 1977; Stilbs, 1986), using either a Bruker 322s NMR spectrometer equipped with an iron-core magnet operating at 60 MHz for protons or a Bruker MSL 100 FT NMR spectrometer equipped with a 2.35-T superconducting magnet. A pair of identical gradient pulses of constant magnitude g and separation Δ and varying width δ was applied at each side of the 180° radio-frequency pulse in a 90°–τ–180° Hahn spin-echo sequence.

The echo amplitude E at time 2τ is a weighted sum of contributions from all proton-bearing components in the system. For a sample containing only one proton-bearing component the echo amplitude at time 2τ is attenuated according to

$$E/E_0 = \exp[-(\gamma g\delta)^2(\Delta - \delta/3)D] \quad (1)$$

where γ is the magnetogyric ratio and D is the diffusion coefficient (Stejskal & Tanner, 1965). A fit of eq 1 to the echo amplitude as a function of δ gives the diffusion coefficient, provided that the value of g is known. For a sample with several proton-bearing diffusing components, the individual diffusion coefficients may be obtained after Fourier transformation of one-half of the spin echo followed by a fit of eq 1 to the signal amplitudes in the frequency domain spectra as functions of δ (Stilbs, 1986). For a system with species differing greatly in the magnitude of D, the diffusion coefficient of the most slowly diffusing component can be obtained from a fit of eq 1 to the latter part of the echo attenuation curve in the time domain.

Thus, in cubic-phase samples of PE and PC treated with heavy water to remove exchangeable protons, the lipid diffusion coefficient was obtained from the time domain echo amplitude as a function of δ. Equation 1 was well fitted to the echo attenuation curve, which indicated that the diffusion coefficients of PE and PC are of very similar magnitude. The water diffusion coefficient in cubic-phase samples was obtained from the amplitude of the water peak in the frequency domain NMR spectra as a function of δ. The lipid diffusion coefficient in the DPG–dibucaine–Tris–HAc–EDTA–NaCl–^2H_2O samples was obtained from the last part of the echo attenuation curve.

With the Bruker 322s system, the echo amplitude was measured from an oscilloscope display of single scans, while with the Bruker MSL 100 system a multiple of four scans was accumulated in quadrature mode, followed either by Fourier transformation of one-half of the echo or by digital phase correction for maximum echo amplitude in the time domain.

The magnetic field gradients were generated with a home-built fully digitized pulsed magnetic field gradient unit or with a slightly modified Bruker B-Z 18 B gradient unit for the Bruker 322s and the Bruker MSL 100 systems, respectively. The magnitude of the field gradient pulses were determined by measurements on doubly distilled water or on water-free glycerol, whose diffusion coefficients are known from the literature (Mills, 1973; Tomlinson, 1973). For water diffusion measurements g was 0.18 Tm^{-1}, and for lipid diffusion measurements g was 1.50 Tm^{-1} (Bruker 322 s) and 1.24 Tm^{-1} (Bruker MSL 100). A typical setting for τ was between 18 and 50 ms. Separation, Δ, was set to 1.3 times τ and δ was varied from 1 ms to at most 14 ms, depending on the value of the diffusion coefficient. Generally, the echo amplitude was followed through one decade of attenuation.

X-ray Diffraction. X-ray diffraction studies of the cubic liquid-crystalline phases were performed in the manner previously reported (Lindblom et al., 1979; Arvidson et al., 1985).

Table II: Measured Values for the Water Translational Diffusion Coefficient in Bicontinuous Cubic Lipid–Water Phases[a]

sample	compn (wt %)	temp (°C)	$D \times 10^9$ ($m^2 \cdot s^{-1}$)	D_{H_2O}/D
monoolein	73	20	0.44	4.7
^1H_2O	27	26	0.50	4.7
		32	0.58	4.7
POPC[b]	6.4	7	0.26	4.3
DLiPE	56.3	13	0.35	3.9
^2H_2O	37.3			
POPC[b]	6.0	20	0.40	4.2
DLiPE	53.0	26	0.59	3.4
^2H_2O	41.0	32	0.71	3.2
DPG[c]	42	7	0.22	5.0
dibucaine	17	13	0.30	4.6
^2H_2O	41			

[a] D, the diffusion of ^1H_2O in the cubic phase; D_{H_2O}/D, the ratio between the diffusion of ^1H_2O in pure water and in the cubic phase. In the samples prepared with ^2H_2O the diffusion of trace amounts of ^1H_2O in ^2H_2O was measured. When calculating D_{H_2O}/D in these cases it was taken into account that the diffusion of trace amounts of ^1H_2O in ^2H_2O is slower than in ^1H_2O (Mills, 1973). No excess water was present in the lipid–water mixtures studied. The water diffusion coefficients thus represent diffusion of water molecules *within* the cubic-phase structure. [b] ^2H_2O contained 100 mM NaCl. [c] ^2H_2O contained 50 mM Tris–HAc (p^{2}H 7.2), 100 mM NaCl, and 2 mM EDTA.

Results

Water Diffusion in a Cubic Phase of Monoolein–Water. Monoolein forms a bicontinuous cubic phase together with water (for references, see the introduction). The water diffusion coefficient in a sample with 27% (w/w) ^1H_2O was found to be approximately a factor of 5 smaller than in pure water at the same temperature (Table II). A reduction of the water diffusion coefficient, as compared to pure water, is to be expected in a cubic phase with a continuous water region: first, the water molecules are confined to move within the water channels formed by the lipid aggregates, and second, the observed water diffusion is slowed down by the association of water molecules to the polar head groups.

Cubic Phases with DOPC–DOPE–^2H_2O and POPC–DLiPE–^2H_2O. Some lipid–water mixtures giving freeze–fracture replicas with three-dimensional regular arrays of "lipidic particles" contain one lipid forming a lamellar phase and one lipid forming a reversed hexagonal (H_{II}) phase, when mixed alone with water. Examples of such a system are mixtures containing PC and PE with unsaturated acyl chains (Hui & Boni, 1982; Hui et al., 1983; Boni & Hui, 1983). In this study POPC, DOPC, DOPE, and DLiPE were used; the PC species form a lamellar phase and the PE species form an H_{II} phase in excess water, respectively (Boni & Hui, 1983; Gutman et al., 1984; Cullis & De Kruijff, 1978).

The phase equilibria in some DOPC–DOPE–^2H_2O mixtures have been investigated (Eriksson et al., 1985a). Mixtures with 50, 63, and 73 mol % DOPC, and with 10% H_2O (w/w), form a cubic liquid-crystalline phase at temperatures above 65, 75, and 85 °C, respectively. At lower temperatures these mixtures form a lamellar phase. The cubic phase was optically isotropic when viewed between two crossed polarizers [according to Rosevear (1954)] and gave very narrow, isotropic peaks in the NMR spectra. The ^{31}P NMR spectra each consisted of two peaks (Figure 2), since the phosphorus nuclei in DOPC and DOPE have different chemical shifts (Eriksson et al., 1985a).

For determination of the lateral diffusion coefficient in a lamellar phase, the lipid–water mixture has to be macroscopically aligned between glass plates and put at the so-called "magic angle" in the magnetic field (Lindblom &

Table III: Measured and Calculated Values for the Lipid Translational Diffusion Coefficient in Bicontinuous Cubic Lipid–Water Systems[a]

sample	compn (wt %)	phase	temp (°C)	$D^{lam} \times 10^{12}$ ($m^2 \cdot s^{-1}$)	$D^{cub} \times 10^{12}$ ($m^2 \cdot s^{-1}$)	$D_L^{cub} \times 10^{12}$ ($m^2 \cdot s^{-1}$)	$D_\parallel^{cub} \times 10^{12}$ ($m^2 \cdot s^{-1}$)
DOPC	46.2	lamellar	36	3.0			
DOPE	43.8		46	3.4			
^2H_2O	10.0		56[b]	5.8			
		cubic	66		3.7	5.6	11.2
			73		5.0	7.5	14.9
			83		6.4	9.6	19.2
			90		7.8	11.8	23.5
DOPC	57.9	cubic	94		7.2	10.8	21.6
DOPE	32.1						
^2H_2O	10.0						
DOPC	66.2	cubic	98		7.4	11.1	22.2
DOPE	23.8						
^2H_2O	10.0						
POPC[c]	7.3	cubic	20		1.6	2.4	4.8
DLiPE	63.9						
^2H_2O	28.8						
POPC[c]	9.6	cubic	20		1.8	2.7	5.4
DLiPE	53.1						
^2H_2O	37.3						
POPC[c]	6.4	cubic	20		1.9	2.9	5.7
DLiPE	56.3						
^2H_2O	37.3						
POPC[c]	6.0	cubic	23		2.6	3.9	7.8
DLiPE	53.0		27		3.1	4.7	9.3
^2H_2O	41.0		33		4.4	6.6	13.2
			40		5.8	8.7	17.4
			46		7.4	11.1	22.2
DPG[d]	42	cubic	19		0.6	0.9	1.8
dibucaine	17						
^2H_2O	41						

[a] For explanation of D^{lam}, D^{cub}, D_L^{cub}, and $D_\parallel^{cub}$, see footnotes to Table I. [b] The presence of an H_{II} phase in the sample does not influence the measured lateral diffusion coefficient in the lamellar phase. [c] ^2H_2O contained 100 mM NaCl. [d] ^2H_2O contained 50 mM Tris–HAc (p^2H 7.2), 100 mM NaCl, and 2 mM EDTA.

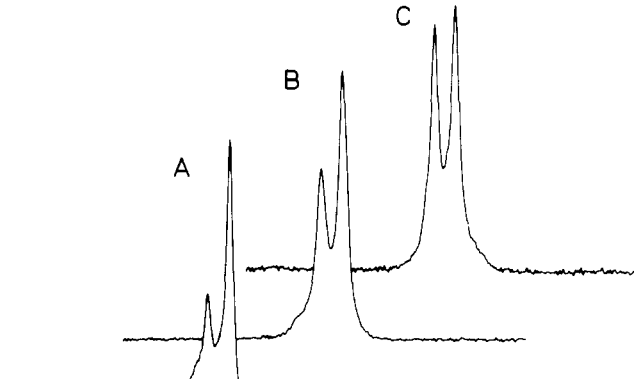

FIGURE 2: 101.3-MHz ^{31}P NMR spectra of the cubic phase formed by different DOPC–DOPE mixtures at constant ^2H_2O content (10% w/w): (A) molar ratio DOPC/DOPE = 73/27, 90 °C; (B) molar ratio DOPC/DOPE = 63/37, 90 °C; and (C) molar ratio DOPC/DOPE = 50/50, 80 °C. The difference in isotropic chemical shift between DOPC and DOPE is 0.73 ppm.

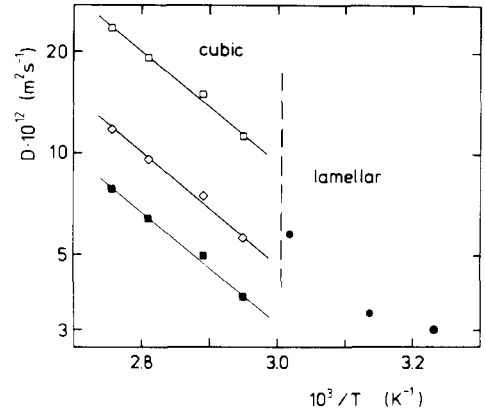

FIGURE 3: Lipid translational diffusion coefficients in the lamellar (●) and cubic (■) phases formed by a sample with a DOPC/DOPE molar ratio of 1.0 and with 10% ^2H_2O (w/w). Filled symbols refer to the measured diffusion coefficients and open symbols to the calculated *local* diffusion coefficients (Lindblom & Wennerström, 1977; Lindblom et al., 1979) in a bicontinuous cubic phase consisting of lamellar units (Lindblom et al., 1979) (◇) and rod-shaped units (Luzzati et al., 1968) (□), respectively.

Wennerström, 1977). The sample containing 50 mol % DOPC was treated in this way, and the lipid diffusion was measured in both the lamellar phase and the cubic phase (Table III; Figure 3). The measured diffusion coefficient (filled symbols) increases with temperature, and it is of the same order of magnitude in both phases. There is a small decrease in the diffusion coefficient at the transition between the lamellar phase and the cubic phase, but this decrease can be explained by the confinement of the lipid molecules to the three-dimensionally folded surfaces in a bicontinuous cubic phase (Lindblom & Wennerström, 1977; Lindblom et al., 1979). A cubic phase composed of closed aggregates, like reversed spherical micelles, would give a measured lipid diffusion coefficient at least 1 order of magnitude lower than the one observed (Table I). In the samples with 63 and 73 mol % DOPC the diffusion was measured only in the cubic phase (Table III); the coefficients are almost the same as those

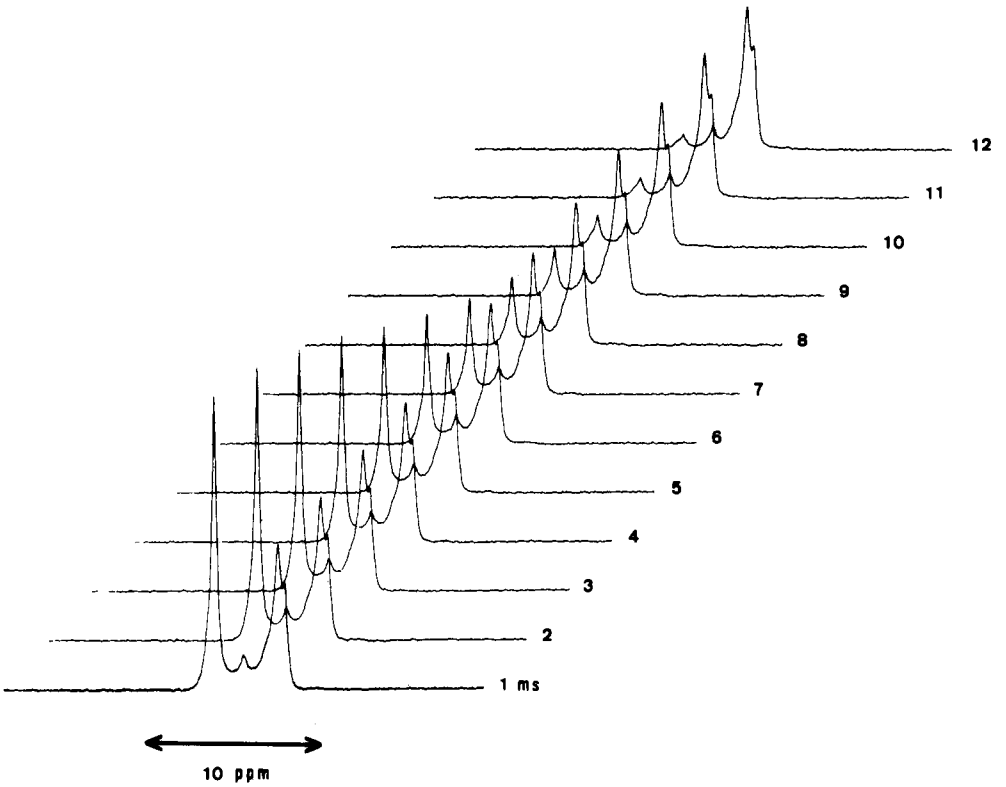

FIGURE 4: Stacked-plot representation of ^1H NMR spectra obtained from a Fourier transform of the second half of the spin echo in an NMR diffusion experiment (see Materials and Methods). The length of the gradient pulse (δ) was increased from 1 to 12 ms. τ = 30 ms, Δ = 40 ms, and g = 0.18 Tm^{-1}. The sample was a cubic phase of POPC–DLiPE–^2H_2O with a molar ratio POPC/DLiPE = 10/90 and with 37.3% (w/w) ^2H_2O containing 100 mM NaCl and trace amounts of ^1H_2O. The spectra were recorded at 7 °C. Due to the fast diffusion of water in the cubic phase, the water peak amplitude decreased strongly with increasing values of δ, whereas the peaks from the slower diffusing lipids decreased very weakly. A fit of eq 1 to the water peak amplitudes gives $D = 2.6 \times 10^{-10}$ $m^2 \cdot s^{-1}$ (Table II).

obtained with the sample containing 50 mol % DOPC. These results show that both the hydrocarbon and the water regions in the cubic phase of DOPC–DOPE–^2H_2O are continuous; i.e., the cubic phase is bicontinuous.

No freeze–fracture electron micrographs are available from the cubic phase of DOPC–DOPE–^2H_2O. However, such micrographs exist from the cubic phases formed by the systems egg PC–DLiPE–H_2O and POPC–DLiPE–H_2O (Hui et al., 1983; Boni & Hui, 1983). In this study the lipid and water diffusion coefficients were determined in four different POPC–DLiPE–^2H_2O mixtures forming a cubic phase. The measured lipid diffusion coefficient in a sample containing 41 wt % ^2H_2O varied from 2.6×10^{-12} $m^2 \cdot s^{-1}$ at 23 °C to 7.4×10^{-12} $m^2 \cdot s^{-1}$ at 46 °C (Table III). These values are somewhat higher than those obtained for the *lamellar* phase of DOPC–DOPE–^2H_2O with 50 mol % DOPC (Table III) and slightly lower than those obtained for the *lamellar* phase of DOPC–^2H_2O (Table I). The lipid diffusion coefficient is slightly raised when the water content in the cubic phase of POPC–DLiPE–^2H_2O is increased (Table III). The diffusion coefficient of water in this cubic phase is about 3–4 times slower than in pure water (Table II; Figure 4). Thus, the water diffusion is retarded to about the same extent in the cubic phase of POPC–DLiPE–^2H_2O and in the bicontinuous cubic phase of monoolein–water, as compared to pure water.

Freeze–fracture electron micrographs from the cubic phases of egg PC–DLiPE–H_2O and POPC–DLiPE–H_2O exhibit three-dimensional arrays of "lipidic particles" (Figure 5a,b; Hui et al., 1983; Boni & Hui, 1983). Hui and colleagues concluded that these cubic phases are built up of reversed micelles with "possible interconnections". However, the results obtained in this study demonstrate that the cubic phases formed by the systems DOPC–DOPE–^2H_2O and POPC–DLiPE–^2H_2O do not consist of closed lipid aggregates, such as reversed micelles; the hydrocarbon regions as well as the water regions must be continuous, since both the lipid and the water molecules are able to diffuse over macroscopical distances.

Cubic Phase with DPG–Dibucaine–^2H_2O. This system belongs to group 3 mentioned in the introduction and is able to form three-dimensional arrays of "lipidic particles" (Figure 5c; Cullis et al., 1978).

DPG–^2H_2O mixtures containing 35 and 50 wt % ^2H_2O gave ^{31}P NMR spectra with a low-field shoulder and a high-field peak (Figure 6a); such spectra are characteristic for a lamellar liquid-crystalline phase (McLaughlin et al., 1975). The chemical shift anisotropy was approximately −34 ppm, which is in agreement with the values reported earlier (Cullis et al., 1978; De Kruijff et al., 1982).

Addition of the local anesthetic dibucaine to the DPG–^2H_2O system induces the formation of nonlamellar phases (Cullis et al., 1978). A DPG–dibucaine–^2H_2O mixture with a dibucaine/DPG ratio of 1.5 and with 41 wt % ^2H_2O containing buffer components, NaCl and EDTA (see Materials and Methods), formed an isotropic liquid-crystalline phase at temperatures between 0 and 20 °C. The phase was optically isotropic when viewed between two crossed polarizers [according to Rosevear (1954)], and ^{31}P NMR spectra exhibited narrow symmetrical peaks (Figure 6b–d). The isotropic phase was also studied with X-ray diffraction at 4 °C (Table IV). The reflections were somewhat diffuse, and it was not possible to unambiguously determine the space group. However, the reflections can be indexed in a primitive cubic lattice with a unit cell dimension of approximately 146 Å. The isotropic phase formed by the above-mentioned DPG–dibucaine–^2H_2O mixture is thus a cubic liquid-crystalline phase. This phase

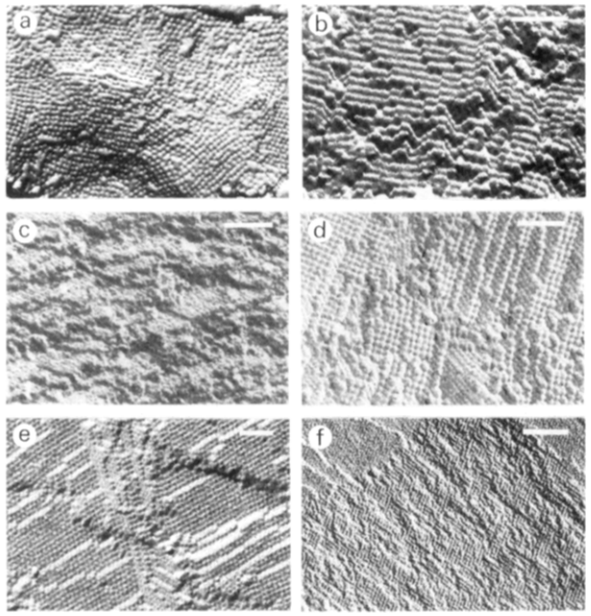

FIGURE 5: Freeze–fracture electron micrographs of different lipid–water mixtures exhibiting three-dimensional regular arrays of "lipidic particles" (a–e) and parallel striations (f). (a) DLiPE–egg PC (molar ratio 85/15) dispersed in a water solution containing buffer, NaCl, and histidine. The sample was quenched from 22 °C after being heated to 40 °C. Reprinted from Hui et al. (1983). (b) DLiPE–POPC (molar ratio 95/5) dispersed in a water solution containing buffer, NaCl, EDTA, and histidine. The sample was quenched from 20 °C. Reprinted from Boni and Hui (1983). (c) DPG–dibucaine (molar ratio 1/1.5) dispersed in a heavy-water solution containing buffer, NaCl, and EDTA. The sample was quenched from 0 °C. Reprinted from Cullis et al. (1978). (d) MGalDG–DGalDG (2:1 w/w) dispersed in a water solution containing NaCl. The sample was quenched from 50 °C. Reprinted from Sprague and Stachelin (1984). (e) Dioleoyl-MGluDG–dioleoyl-DGluDG–^2H_2O with a molar ratio MGluDG/DGluDG of 3.0 and with excess ^2H_2O. The sample was quenched from 50 °C. From Å. Wieslander, unpublished results. (f) Dioleoyl-MGluDG–^2H_2O with 9 wt % ^2H_2O. The sample was quenched from 20 °C. Reprinted from Lindblom et al. (1986). White bars represent 100 nm.

Table IV: X-ray Diffraction Results for the Cubic Phase in the System DPG–Dibucaine–^2H_2O (See Text) at 4 °C

mm	$h^2 + k^2 + l^2$	d^a (Å)	a^b (Å)
10.5	6	60.1	147.2
12.0	8	52.6	148.7
15.5	13	40.7	146.8
16.5	14	38.2	143.1
18.5	18	34.1	144.7
19.5	21	32.3	148.3

[a] d is the Bragg spacing. [b] a is the cubic unit cell dimension.

gradually transformed into a hexagonal phase (probably H_{II}) above 20 °C, as judged by the ^{31}P NMR spectra exhibiting a low-field peak and a high-field shoulder (McLaughlin et al., 1975); the value of the chemical shift anisotropy was about one-half the value obtained from the lamellar phase of DPG–^2H_2O (Figure 6e,f).

The lipid translational diffusion coefficient in the cubic liquid-crystalline phase was measured to be 0.6×10^{-12} m^2·s^{-1} at 19 °C (Table III). When this value is corrected for geometrical factors (Lindblom & Wennerström, 1977; Lindblom et al., 1979), a translational diffusion coefficient of 0.9×10^{-12} or 1.8×10^{-12} m^2·s^{-1} is obtained. The sample forming the cubic phase does not form a lamellar phase above 0 °C (Figure 6), and it is thus impossible to determine the lipid lateral diffusion coefficient in a lamellar phase with the above-mentioned composition. However, the diffusion coefficient in the cubic phase can instead be compared to the lipid lateral diffusion

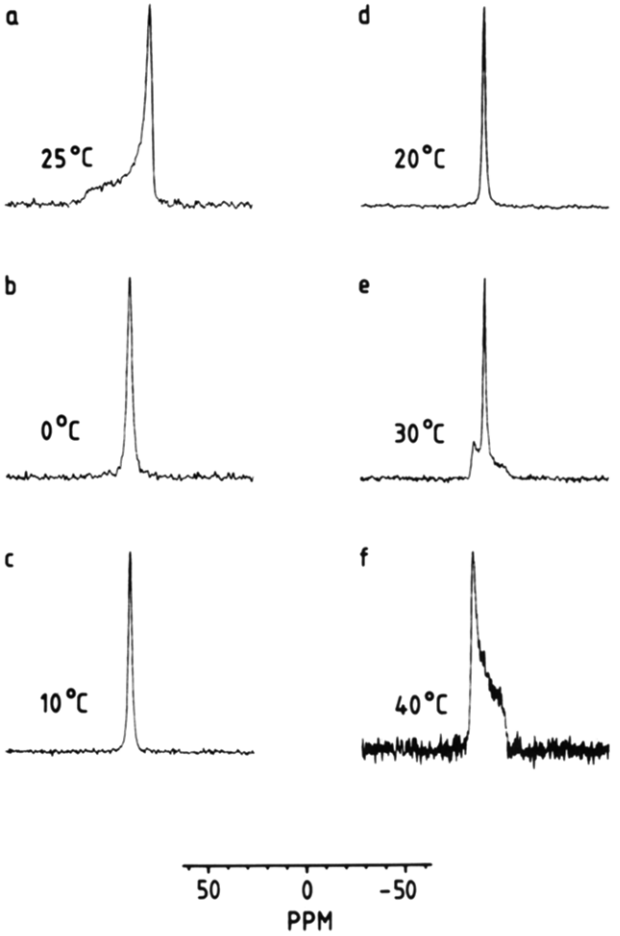

FIGURE 6: 40.5-MHz ^{31}P NMR spectra of (a) a DPG–^2H_2O mixture with 50 wt % ^2H_2O and (b–f) a DPG–dibucaine–^2H_2O mixture with a molar ratio dibucaine/DPG of 1.5 and with 41 wt % ^2H_2O containing buffer, NaCl, and EDTA (see Materials and Methods).

coefficient of DOPC in the lamellar phase, which is 2.8×10^{-12} m^2·s^{-1} at 20 °C (Table I; Lindblom et al., 1981). It should be noted that the diffusion coefficient in the cubic phase of DPG–dibucaine–^2H_2O shall be compared to the diffusion coefficient in a lamellar phase formed by a biological membrane lipid, with two acyl chains and a large polar head group, and not to the diffusion coefficient in a lamellar phase formed by a surfactant molecule, with one acyl chain and a small polar head group (Table I). Accordingly, the lipid diffusion in the cubic phase of DPG–dibucaine–^2H_2O is found to be very close to that in a lamellar phase formed by a biological membrane lipid. Moreover, the measured lipid translational diffusion at 19 °C in the cubic phase of DPG–dibucaine–^2H_2O is 10 times faster than the lipid translational diffusion at 29 °C in the cubic phase of LaLPC–^2H_2O (Tables I and III), which is built up by closed lipid aggregates.

The water diffusion coefficient in the cubic phase of DPG–dibucaine–^2H_2O was measured at 7 and 13 °C (Table II). The reduction in the coefficient as compared to pure water is nearly the same as in the bicontinuous cubic phases of POPC–DLiPE–^2H_2O and monoolein–water. Thus, the water molecules are not confined to closed compartments. All the above-mentioned results lead to the conclusion that the cubic phase of DPG–dibucaine–^2H_2O is bicontinuous. This phase has previously been classified as an intermediate phase built up by "regions of short hexagonal (H_{II}) phase" (Cullis et al., 1978). This classification implies that the phase consists of closed lipid aggregates. However, it is shown here that, first, the intermediate phase is a *cubic* liquid-crystalline phase and,

second, the cubic phase is *bicontinuous*.

Discussion

In this study the lipid and water translational diffusion coefficients were determined in the cubic phases formed by the three systems DOPC–DOPE–^2H_2O, POPC–DLiPE–^2H_2O, and DPG–dibucaine–^2H_2O. Freeze–fracture electron micrographs showing three-dimensional arrays of "lipidic particles" have been obtained from the two latter systems. From our results we conclude that, in these cubic phases, both the lipid and the water molecules can diffuse over macroscopical distances. Thus, both the hydrocarbon and the water regions are continuous; i.e., the cubic phases are bicontinuous.

The lipid translational diffusion coefficient has been determined for several cubic phases formed by biological lipids, and some of these phases have also been studied with freeze–fracture electron microscopy.

Galactolipid–water mixtures with a molar ratio MGalDG/DGalDG between 0.7 and 2.0 have yielded freeze–fracture images with three-dimensional arrays of "lipidic particles" (Figure 5d; Sen et al., 1982; Sprague & Staehelin, 1984). Sen et al. (1982) proposed that these electron micrographs show quasi-crystalline or crystallike arrangements of particles corresponding to reversed lipid micelles. Sprague and Staehelin (1984) discovered central holes in some of the particles and discussed the possibility that these holes may reflect regions of contact between (1) reversed micelles in adjacent planes or (2) bilayer vesicles joined together as in a prolamellar body. However, these interpretations were judged as unlikely, and the "lipidic particles" were finally proposed to represent pure reversed micelles (Sprague & Staehelin, 1984). X-ray diffraction studies have revealed that galactolipid–water mixtures with the above-mentioned MGalDG/DGalDG ratios can form a reversed cubic liquid-crystalline phase belonging to the space group *Ia3d* (Rivas & Luzzati, 1969; Brentel et al., 1985). From measurements of the lipid translational diffusion coefficient in the cubic phase, it was concluded that this phase is bicontinuous (Brentel et al., 1985). This conclusion is given some support by the observation of central holes in the "lipidic particles" (Sprague & Staehelin, 1984).

Mixtures of dioleoyl-MGluDG, dioleoyl-DGluDG, and ^2H_2O are able to form a reversed cubic liquid-crystalline phase (Wieslander et al., 1981; Khan et al., 1981). Freeze–fracture electron micrographs of this phase exhibit a three-dimensional array of "lipidic particles" (Figure 5e; Å. Wieslander, unpublished results), and from measurements of the lipid diffusion coefficient in the lamellar and the cubic phases, the conclusion was drawn that the cubic phase is bicontinuous (Wieslander et al., 1981; Lindblom et al., 1986).

A cubic phase is located between the lamellar and H_{II} phases in the phase diagrams of many monoglyceride–water systems (Lutton, 1965; Lindblom et al., 1979; Longley & McIntosh, 1983; Larsson, 1983; Hyde et al., 1984). An NMR diffusion experiment, like the one shown in Figure 3, with the cubic phase of monoolein–water clearly demonstrated that the lipids can diffuse over macroscopical distances (Table I; Lindblom et al., 1979). Freeze–fracture images of a cubic phase formed by sunflower oil monoglyceride–water mixtures show a three-dimensional array of globular elements arranged in a body-centered lattice, if the phase structure is stabilized by cytochrome *c* dissolved in the water (Gulik-Kryzwicki et al., 1984).

A cubic phase formed by egg LPC and water, located between the isotropic micellar solution and the normal hexagonal (H_I) phase, has been investigated with the freeze–fracture technique (Gulik-Krzywicki et al., 1984). The electron micrographs reveal three-dimensional arrays of globular elements that display square symmetry. A novel phase structure for cubic phases with this location in the phase diagram was recently presented (Fontell et al., 1985): rod-shaped micelles of the *normal* type, with an axial ratio around 2, occupy two nonequivalent positions in the cubic unit cell (Fontell et al., 1985; Eriksson et al., 1985b). The cubic phases at this location in the phase diagram in the systems C_{12}TACl–water and LaLPC–water are also proposed to have this structure (Fontell et al., 1985; Eriksson et al., submitted for publication). Measurement of the lipid translational diffusion coefficient showed that these phases are composed of closed lipid aggregates (Table I; Bull & Lindman, 1974; Eriksson et al., 1982, submitted for publication). Moreover, the water diffusion in the cubic phase of LaLPC–^2H_2O was found to be only a factor of 2.7 slower than in pure water (Eriksson et al., submitted for publication). Thus, the diffusion data are in agreement with the proposed structure of these cubic phases. In this case regular arrays of "lipidic particles" are obtained from a cubic liquid-crystalline phase composed of *closed* lipid aggregates of the *normal* type.

A dioleoyl–MGluDG–^2H_2O mixture can form a cubic liquid-crystalline phase which belongs to the space group *Ia3d* (Lindblom et al., 1986). The lipid translational diffusion coefficient has been determined for this phase, and it shows that the phase is bicontinuous (Lindblom et al., 1986). However, the freeze–fracture image of this phase differs from the above-mentioned images and instead exhibits parallel striations where the individual "lipidic particles" are indicated but not clearly resolved (Figure 5f; Lindblom et al., 1986). Similar freeze–fracture replicas have been obtained from the cubic phase formed by the system egg PC–water (Gulik-Krzywicki et al., 1984) and sometimes also from MGalDG–DGalDG–water mixtures (Sen et al., 1982); replicas from the latter system were described to have a "herringbone" pattern.

Conclusions

Freeze–fracture replicas of several lipid–water mixtures show three–dimensional regular arrays of "lipidic particles". Many of the phases yielding such replicas have been poorly classified with respect to long-range organization and symmetry and have been suggested to be built up by closely packed reversed micelles. However, it has been shown in many cases that these phases in reality are *cubic* liquid-crystalline phases, according to the established classification of lyotropic liquid-crystalline phases. Among the cubic phases giving three-dimensional arrays of "lipidic particles", and whose phase structures are known, all phases except one are *bicontinuous*; i.e., both the hydrocarbon and the water regions are continuous. The exception is a cubic phase composed of *closed* rod-shaped micelles of the *normal* type. Hence, it is not possible to decide from freeze–fracture replicas of a cubic phase, showing three-dimensional arrays of "lipidic particles", if the phase is bicontinuous or built up by closed lipid aggregates. In addition, some bicontinuous cubic phases exhibit freeze–fracture images that differ from the above-mentioned images; the alternative structures are described as parallel striations or "herringbone" patterns, in which the individual "lipidic particles" are indicated but not distinctly resolved.

From the results discussed in this paper we conclude that, hitherto, it has not been demonstrated that a biological membrane lipid–water system is able to form a cubic liquid-crystalline phase consisting of reversed micelles. This statement is comprehensible, considering the location in the phase diagrams of the cubic phases formed by biological membrane

lipids. Cubic phases may in principle have the following locations in a binary lipid–water phase diagram (Fontell, 1981): (1) between the isotropic micellar solution and the H_I phase; (2) between the H_I and lamellar phases; (3) between the lamellar and H_{II} phases; and (4) between the H_{II} phase and the reversed micellar phase. In the phase diagrams of three-component systems, like some of the systems described above, there are still more locations that are possible. It has also been asserted that the structure of the aggregates building up the various cubic phases must be in a logical relation to the aggregate structures of the neighboring phases (Fontell, 1981). Thus, cubic phases with location 1 are composed of closed aggregates of the normal type; examples of such phases are C_{12}TACl–water with 50 wt % water and LaLPC–water (Table I). In contrast, cubic phases located between the H_I and the lamellar phases are bicontinuous. NMR diffusion measurements indicate that these phases (for example sodium diethylhexylsulfosuccinate–water, C_{12}TACl–water with 16 wt % water, and OlLPC–water) are built up by rod-shaped or lamellar aggregates (Table I; Lindblom et al., 1979). If we then turn to the cubic phases of the reversed type, the phases with location 3 should, for symmetry reasons, be bicontinuous and consist of rod-shaped or lamellar aggregates. The cubic phases formed by biological membrane lipid–water systems seem to have this location in the phase diagrams (Rilfors et al., 1984), and the phase structures proposed for these phases are in fact built up by rod-shaped or lamellar aggregates (Luzzati et al., 1968; Lindblom et al., 1979; Gulik et al., 1985). According to this line of reasoning, cubic phases consisting of reversed micelles should be located between the H_{II} phase and the reversed micellar phase. However, the existence of cubic phases that with certainty have location 4 in phase diagrams has not been demonstrated in *any* lipid–water system (Fontell, 1981). In the light of the above-mentioned considerations, the suggestion put forward by Verkleij (1984), that the transition between a lamellar and an H_{II} phase proceeds via, firstly, a bicontinuous cubic phase composed of lamellar aggregates and, secondly, a cubic phase built up by reversed micelles, therefore seems improbable.

Finally, theoretical calculations of the phase equilibria in PE–phosphatidylserine–water systems have been presented (Kirk et al., 1984). Three phase structures were considered: a lamellar phase, a cubic phase composed of closely packed reversed spherical micelles, and an H_{II} phase. The phosphatidylserine content was varied from 0% to 60%, and the phase transitions as a function of the water content in the systems were calculated. The cubic phase was never predicted to have the lowest total free energy. Thus a cubic phase consisting of reversed spherical micelles was not found to be a stable structure in these lipid–water systems.

ACKNOWLEDGMENTS

We thank Krister Fontell for performing the X-ray diffraction study of the DPG–dibucaine–^2H_2O cubic phase.

Registry No. C_{12}TACl, 112-00-5; LaLPC, 20559-18-6; OlLPC, 19420-56-5; DOPC, 10015-85-7; POPC, 6753-55-5; DLiPE, 55252-82-9; DOPE, 2462-63-7; $Bu(CH_2)_3CO_2H$, 124-07-2; $Bu(CH_2)_6OH$, 112-30-1; $Bu(CH_2)_3Me$, 111-65-9; monoolein, 25496-72-4; dibucaine, 85-79-0.

REFERENCES

Arvidson, G., Brentel, I., Khan, A., Lindblom, G., & Fontell, K. (1985) *Eur. J. Biochem. 152*, 753–759.

Boni, L. T., & Hui, S. W. (1983) *Biochim. Biophys. Acta 731*, 177–185.

Brentel, I., Selstam, E., & Lindblom, G. (1985) *Biochim. Biophys. Acta 812*, 816–826.

Bull, T., & Lindman, B. (1974) *Mol. Cryst. Liq. Cryst. 28*, 155–160.

Charvolin, J., & Rigny, P. (1971) *J. Magn. Reson. 4*, 40–46.

Comfurius, P., & Zwaal, R. F. A. (1977) *Biochim. Biophys. Acta 488*, 36–42.

Cullis, P. R., & De Kruijff, B. (1978) *Biochim. Biophys. Acta 513*, 31–42.

Cullis, P. R., Verkleij, A. J., & Ververgaert, P. H. J. T. (1978) *Biochim. Biophys. Acta 513*, 11–20.

Dekker, C. J., Geurts van Kessel, W. S. M., Klomp, J. P. G., Pieters, J., & De Kruijff, B. (1983) *Chem. Phys. Lipids 33*, 93–106.

De Kruijff, B., Verkleij, A. J., Leunissen-Bijvelt, J., Van Echteld, C. J. A., Hille, J., & Rijnbout, H. (1982) *Biochim. Biophys. Acta 693*, 1–12.

De Kruijff, B., Cullis, P. R., Verkleij, A. J., Hope, M. J., Van Echteld, C. J. A., & Taraschi, T. F. (1985) in *Enzymes of Biological Membranes* (Martinosi, A., Ed.) pp 131–204, Plenum, New York.

Eriksson, P.-O., Khan, A., & Lindblom, G. (1982) *J. Phys. Chem. 86*, 387–393.

Eriksson, P.-O., Rilfors, L., Lindblom, G., & Arvidson, G. (1985a) *Chem. Phys. Lipids 37*, 357–371.

Eriksson, P.-O., Lindblom, G., & Arvidson, G. (1985b) *J. Phys. Chem. 89*, 1050–1053.

Fontell, K. (1981) *Mol. Cryst. Liq. Cryst. 63*, 59–82.

Fontell, K., Fox, K. K., & Hansson, E. (1985) *Mol. Cryst. Liq. Cryst. 1*, 9–17.

Gulik, A., Luzzati, V., De Rosa, M., & Gambacorta, A. (1985) *J. Mol. Biol. 182*, 131–149.

Gulik-Krzywicki, T., Aggerbeck, L. P., & Larsson, K. (1984) in *Surfactants in Solution* (Mittal, K. L., & Lindman, B., Eds.) Vol. 1, pp 237–257, Plenum, New York.

Gupta, C. M., Radhakrishnan, R., & Khorana, H. G. (1977) *Proc. Natl. Acad. Sci. U.S.A. 74*, 4315–4319.

Gutman, H., Arvidson, G., Fontell, K., & Lindblom, G. (1984) in *Surfactants in Solution* (Mittal, K. L., & Lindman, B., Eds.) Vol. 1, pp 143–152, Plenum Press, New York.

Hui, S. W., & Boni, L. T. (1982) *Nature (London) 296*, 175.

Hui, S. W., Stewart, T. P., & Boni, L. T. (1983) *Chem. Phys. Lipids 33*, 113–126.

Hyde, S. T., Andersson, S., Ericsson, B., & Larsson, K. (1984) *Z. Kristallogr. 168*, 213–219.

Khan, A., Rilfors, L., Wieslander, Å., & Lindblom, G. (1981) *Eur. J. Biochem. 116*, 215–220.

Kirk, G. L., Gruner, S. M., & Stein, D. L. (1984) *Biochemistry 23*, 1093–1102.

Kuo, A.-L., & Wade, C. G. (1979) *Biochemistry 18*, 2300–2308.

Larsson, K. (1983) *Nature (London) 304*, 664.

Lindblom, G., & Wennerström, H. (1977) *Biophys. Chem. 6*, 167–171.

Lindblom, G., Larsson, K., Johansson, L., Fontell, K., & Forsén, S. (1979) *J. Am. Chem. Soc. 101*, 5465–5470.

Lindblom, G., Johansson, L. B.-Å., & Arvidson, G. (1981) *Biochemistry 20*, 2204–2207.

Lindblom, G., Brentel, I., Sjölund, M., Wikander, G., & Wieslander, Å. (1986) *Biochemistry* (in press).

Longley, W., & McIntosh, T. J. (1983) *Nature (London) 303*, 612–614.

Lutton, E. S. (1965) *J. Am. Oil Chem. Soc. 42*, 1068–1070.

Luzzati, V., & Tardieu, A. (1974) *Annu. Rev. Phys. Chem. 25*, 79–94.

Luzzati, V., Gulik-Krzywicki, T., & Tardieu, A. (1968) *Nature (London) 218*, 1031–1034.

McLaughlin, A. C., Cullis, P. R., Berden, J. A., & Richards, R. E. (1975) *J. Magn. Reson. 20*, 146–165.
Mills, R. (1973) *J. Phys. Chem. 77*, 685–688.
Rilfors, L., Lindblom, G., Wieslander, Å., & Christiansson, A. (1984) *Biomembranes 12*, 205–245.
Rivas, E., & Luzzati, V. (1969) *J. Mol. Biol. 41*, 261–275.
Roeder, S. B. W., Burnell, E. E., Kuo, A.-L., & Wade, C. G. (1976) *J. Chem. Phys. 64*, 1848–1849.
Rosevear, F. B. (1954) *J. Am. Oil Chem. Soc. 31*, 628–639.
Scriven, L. E. (1976) *Nature (London) 263*, 123–125.
Sen, A., Williams, W. P., Brain, A. P. R., Dickens, M. J., & Quinn, P. J. (1981) *Nature (London) 293*, 488–490.
Sen, A., Brain, A. P. R., Quinn, P. J., & Williams, W. P. (1982) *Biochim. Biophys. Acta 686*, 215–224.
Sprague, S. G., & Staehelin, L. A. (1984) *Biochim. Biophys. Acta 777*, 306–322.
Stejskal, E. O., & Tanner, J. E. (1965) *J. Chem. Phys. 42*, 288–292.
Stilbs, P. (1986) *Prog. Nucl. Magn. Reson. Spectrosc.* (in press).
Stilbs, P., Arvidson, G., & Lindblom, G. (1984) *Chem. Phys. Lipids 35*, 309–314.
Tomlinson, D. J. (1973) *Mol. Phys. 25*, 735–738.
Van Venetië, R., & Verkleij, A. J. (1981) *Biochim. Biophys. Acta 645*, 262–269.
Verkleij, A. J. (1984) *Biochim. Biophys. Acta 779*, 43–63.
Verkleij, A. J., Mombers, C., Leunissen-Bijvelt, J., & Ververgaert, P. H. J. T. (1979) *Nature (London) 279*, 162–163.
Verkleij, A. J., De Maagd, R., Leunissen-Bijvelt, J., & De Kruijff, B. (1982) *Biochim. Biophys. Acta 684*, 255–262.
Wieslander, Å., Rilfors, L., Johansson, L. B.-Å., & Lindblom, G. (1981) *Biochemistry 20*, 730–735.

Ether Phosphatidylcholines: Comparison of Miscibility with Ester Phosphatidylcholines and Sphingomyelin, Vesicle Fusion, and Association with Apolipoprotein A-I†

Barry J. McKeone,* Henry J. Pownall, and John B. Massey

Department of Internal Medicine, Baylor College of Medicine and The Methodist Hospital, Houston, Texas 77030

Received June 19, 1986; Revised Manuscript Received August 14, 1986

ABSTRACT: Nonhydrolyzable matrices of ether-linked phosphatidylcholines (PCs) and sphingomyelin have been used to study the mechanism of action of lipolytic enzymes. Since ether PCs, sphingomyelin, and ester PCs vary in the number of hydrogen bond donors and acceptors in the carbonyl region of the bilayer, we have examined several physical properties of ether PCs and sphingomyelin in model systems to validate their suitability as nonhydrolyzable lipid matrices. The intermolecular interactions of ether PCs with ester PCs, sphingomyelin, and cholesterol were investigated by differential scanning calorimetry. Phase diagrams constructed from the temperature dependence of the gel to liquid-crystalline phase transition of 1,2-*O*-dihexadecyl-*sn*-glycero-3-phosphocholine (DPPC-ether) and 1,2-*O*-ditetradecyl-*sn*-glycero-3-phosphocholine (DMPC-ether) with both 1,2-dimyristoyl-*sn*-glycero-3-phosphocholine (DMPC) and 1,2-dipalmitoyl-*sn*-glycero-3-phosphocholine (DPPC) demonstrated complete lipid miscibility in the gel and liquid-crystalline phases. Additionally, phase diagrams of egg yolk sphingomyelin (EYSM) with DMPC or DMPC-ether and 1,2-distearoyl-*sn*-glycero-3-phosphocholine (DSPC) or 1,2-*O*-dioctadecyl-*sn*-glycero-3-phosphocholine (DSPC-ether) demonstrated no major differences in miscibility of EYSM in ester and ether PCs. The effect of 10 mol % cholesterol on the thermal transitions of mixtures of ester and ether PCs also indicates little preference of cholesterol for either lipid. The fusion of small single bilayer vesicles of DMPC, DMPC-ether, DPPC, and DPPC-ether to larger aggregates as determined by gel filtration indicated that the ester PC vesicles were somewhat more stable. The rate of association of apolipoprotein A-I with DMPC or DMPC-ether multilamellar liposomes was compared. The rate was fastest at the gel → liquid-crystalline transition temperature (T_c) of either lipid and was consistent with the insertion of the protein into lattice defects in the lipid matrix. Ether PCs interact with ester PCs, sphingomyelin, cholesterol, and apolipoproteins in a manner similar to ester PCs. The interaction between these lipids appears to be dominated by hydrocarbon chain interactions instead of the hydrogen bonding groups in the carbonyl region. Thus, ether PCs appear to be suitable analogues of the ester PCs for the elucidation of structural–functional mechanisms of lipolysis.

Lipolytic enzymes play an essential role in the metabolism of biological membranes and plasma lipoproteins. Kinetic studies on lipolytic enzymes are difficult to interpret because (a) the processes occur in a heterogeneous medium at a lipid–water interface, (b) the composition and physical properties of the interface are continuously altered by the hydrolysis of the substrate, and (c) the accumulation of lipolytic products can produce subdomains that may have different physical properties (Scanu et al., 1982; Brockman, 1984). To maintain a constant physical state of the lipid–water interface in model substrate systems, nonhydrolyzable lipid matrices of sphin-

† This research was supported by grants from the National Institutes of Health (HL 27341, HL 30913, HL 30914, and T32-HL 07582).

0006-2960/86/0425-7711$01.50/0